

# PERFORMANCE CHARACTERISTICS OF A 1 MV MINIATURE MARX BANK \*

F.E. Peterkin, D.C. Stoudt, B.J. Hankla, K.A. Boulais, J.S. Bernardes  
Naval Surface Warfare Center, Dahlgren Division  
Code B20 / Bldg. 1470  
Dahlgren, VA 22448-5100

## Abstract

In this paper we report results of experiments with a compact Marx bank generator. The Marx was constructed with 25 spark-gap switched stages, each stage consisting of two Murata 2 nF capacitors with N4700 ceramic dielectric rated at 40 kV. In order to evaluate the Marx efficiency and repetition rate, inductive isolation with 5  $\mu$ H per stage was implemented for the charging circuit. The Marx was charged with a 1500 J/s capacitor charging power supply. The system was controlled and monitored with a laptop computer through a fiber optic interface.

We report results from operating the Marx from one quarter to full output voltage, nominal 250 kV to 1 MV open circuit (OC). Short duration testing showed that the Marx could be triggered continuously at a repetition rate varying from 20 to 50 Hz, depending on the charging voltage. Various representative loads were used for diagnostic purposes and for comparison to modeling efforts. When operated into a short circuit, the Marx current oscillated at 14 MHz with a peak amplitude of about 10 kA. The Marx was also operated with and without a coaxial ground enclosure to investigate the influence of this geometry on pulse characteristics. We compare the results of circuit modeling with the experimental measurements and show good agreement.

## I. INTRODUCTION

Many pulsed power applications do not require the large scale equipment and infrastructure necessary for directed energy studies like high power lasers, or fusion experiments like the National Ignition Facility. As a Navy facility, we have a responsibility to investigate pulsed power applications with strong connection to the current and future needs of the naval armed forces and support systems. In light of this mission, we have been able to identify several areas where more compact pulsed power technology has advantages.

These areas are diverse. Ship scale simulations of lightning strikes are often required to validate electronics hardening, but these tests can be cumbersome. The equipment required to simulate a lightning strike must generate potentially 100's of kA and can be difficult to isolate from the system under test. A compact system to simulate the local effects of a lightning strike would be

useful, either through direct current injection or via an electromagnetic coupling mechanism (antenna, induction coil, capacitive).

Another common diagnostic tool for defense applications is the use of flash x-ray measurements to study fast transient phenomena in ballistics and other mechanical events. Marx generators have been used for this application previously. [1]

Applications such as lightning simulation and x-ray production may require only single-shot operation, but there are other interesting uses for compact high-voltage generators which require rep-rate operation.

Recent work has shown that fast-risetime, short-duration electric field pulses can be used effectively to deter the growth of fouling organisms in marine systems and to efficiently sterilize water by killing *e. coli* bacteria.[2] To observe these effects requires pulses with electric field amplitude of the order 10-100 kV/cm, risetime of the order 10 ns, and width ranging from 50 ns to 1  $\mu$ s. In order to treat a chamber of reasonable volume with characteristic dimensions  $\approx$  1-10 cm and filled with low resistivity water at this field amplitude, a generator capable of producing 100's of kV into a relatively low impedance is required. Such a generator must also be capable of rep-rated operation, so that a large volume of material may be treated, typically in a flow-thru geometry.

With these and other applications in mind, we have pursued a program to develop and characterize a miniature Marx bank generator with the potential to be compactly packaged and portably operated. This paper focuses on the operating characteristics of a 1 MV Marx generator based in large part on a design and materials obtained from Los Alamos National Laboratory. We first describe the physical construction of the Marx generator, then provide experimentally measured operating parameters. We conclude with a discussion of a simple circuit model that matches well to the experimental results.

## II. MARX CONSTRUCTION

The Marx generator is pictured in Figure 1. The Marx is constructed from two lexan "spines" each 34 inches long. Thirteen capacitor pairs are mounted on one spine and twelve pairs are mounted on the other, providing 25

\* Work supported by NSWC internal funding. We also gratefully acknowledge the contributions of Dave Platts of Los Alamos National Laboratory for the initial design of the Marx generator and Mike Morgan of the Naval Postgraduate School for the circuit model.

Report Documentation Page				Form Approved OMB No. 0704-0188	
Public reporting burden for the collection of information is estimated to average 1 hour per response, including the time for reviewing instructions, searching existing data sources, gathering and maintaining the data needed, and completing and reviewing the collection of information. Send comments regarding this burden estimate or any other aspect of this collection of information, including suggestions for reducing this burden, to Washington Headquarters Services, Directorate for Information Operations and Reports, 1215 Jefferson Davis Highway, Suite 1204, Arlington VA 22202-4302. Respondents should be aware that notwithstanding any other provision of law, no person shall be subject to a penalty for failing to comply with a collection of information if it does not display a currently valid OMB control number.					
1. REPORT DATE <b>JUN 1999</b>		2. REPORT TYPE <b>N/A</b>		3. DATES COVERED <b>-</b>	
4. TITLE AND SUBTITLE <b>Performance Characteristics Of A 1 Mv Miniature Marx Bank</b>				5a. CONTRACT NUMBER	
				5b. GRANT NUMBER	
				5c. PROGRAM ELEMENT NUMBER	
6. AUTHOR(S)				5d. PROJECT NUMBER	
				5e. TASK NUMBER	
				5f. WORK UNIT NUMBER	
7. PERFORMING ORGANIZATION NAME(S) AND ADDRESS(ES) <b>Naval Surface Warfare Center, Dahlgren Division Code B20 / Bldg. 1470 Dahlgren, VA 22448-5 100</b>				8. PERFORMING ORGANIZATION REPORT NUMBER	
9. SPONSORING/MONITORING AGENCY NAME(S) AND ADDRESS(ES)				10. SPONSOR/MONITOR'S ACRONYM(S)	
				11. SPONSOR/MONITOR'S REPORT NUMBER(S)	
12. DISTRIBUTION/AVAILABILITY STATEMENT <b>Approved for public release, distribution unlimited</b>					
13. SUPPLEMENTARY NOTES <b>See also ADM002371. 2013 IEEE Pulsed Power Conference, Digest of Technical Papers 1976-2013, and Abstracts of the 2013 IEEE International Conference on Plasma Science. Held in San Francisco, CA on 16-21 June 2013. U.S. Government or Federal Purpose Rights License.</b>					
14. ABSTRACT <b>In this paper we report results of experiments with a compact Marx bank generator. The Marx was constructed with 25 spark-gap switched stages, each stage consisting of two Murata 2 nF capacitors with N4700 ceramic dielectric rated at 40 kV. In order to evaluate the Marx efficiency and repetition rate, inductive isolation with 5 uH per stage was implemented for the charging circuit. The Marx was charged with a 1500 J/s capacitor charging power supply. The system was controlled and monitored with a laptop computer through a fiber optic interface. We report results from operating the Marx from one quarter to full output voltage , nominal 250 kV to 1 MV open circuit (OC). Short duration testing showed that the Marx could be triggered continuously at a repetition rate varying from 20 to 50 Hz, depending on the charging voltage. Various representative loads were used for diagnostic purposes and for comparison to modeling efforts. When operated into a short circuit, the Marx current oscillated at 14 MHz with a peak amplitude of about 10 kA. The Marx was also operated with and without a coaxial ground enclosure to investigate the influence of this geometry on pulse characteristics. We compare the results of circuit modeling with the experimental measurements and show good agreement.</b>					
15. SUBJECT TERMS					
16. SECURITY CLASSIFICATION OF:			17. LIMITATION OF ABSTRACT <b>SAR</b>	18. NUMBER OF PAGES <b>4</b>	19a. NAME OF RESPONSIBLE PERSON
a. REPORT <b>unclassified</b>	b. ABSTRACT <b>unclassified</b>	c. THIS PAGE <b>unclassified</b>			



total Marx stages. The capacitor pairs are connected electrically in parallel with brass straps and the straps are mechanically fixed to the spine with bolts and smoothed brass acorn nuts. The nuts are positioned on the inside faces of the spines and located in such a manner that when the two spines are placed together the brass nuts form the 25 spark gap switches used to erect the Marx. The machined dimensions of the spines determine the default spacing of the gaps, but spacers could be used to decrease the gap if necessary. The default spacing was approximately 3 mm.

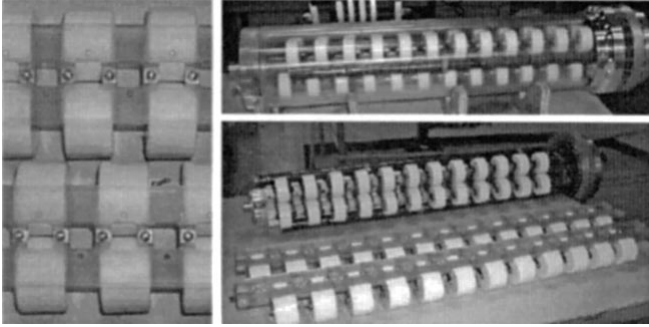


Figure 1. The close-up on the left shows the offset mounting arrangement that allows the strap nuts to serve as spark gap electrodes. The pictures on the right show the Marx in progressive stages of assembly.

We used Murata ceramic capacitors with two different materials and capacitance values, either 2 nF N4700 capacitors or 2.7 nF Z5V capacitors. The Z5V capacitors exhibit a rapid decrease in capacitance with voltage, so that at the rated 40 kV operating limit the capacitance drops to approximately the same level as the N4700 capacitors. The N4700 capacitors have the advantage of lighter weight and smaller size. With 40 kV capacitors and 25 stages, the Marx generated a nominal 1 MV OC.

The lexan spines were bolted together and to an aluminum bulkhead which provided both HV feedthroughs for charging and trigger lines, as well as mechanical mounting of the pressure vessel. The pressure vessel was a single machined cylindrical tube, made of either acrylic or PVC. One end of the tube was closed except for an o-ring sealed feedthrough for the HV output of the Marx. The inner diameter of the tube was 6 inches and the outer diameter 7.5 inches. The other end of the tube was open, to slide over the Marx assembly, and incorporated a flared flange and circle of bolt holes for mounting to the bulkhead. The vessel was pressure tested to 100 PSI.

As we wished to operate this Marx rep-rated, the original design was modified to incorporate an inductive charging path. The inductors are visible in Fig. 1 as the two cylindrical tubes running down the side of the assembled spine. Each inductor was made from 1 inch diameter PVC tube and was wound at 16 thread/inch. Taps come off the inductor periodically to provide the positive and negative charging connections to each side of the capacitor stages. The isolation inductance per stage was measured to vary between 5 and 10  $\mu$ H. This

corresponds to an LC resonance per stage (and in the Marx as a whole when erected) of about 1 MHz.

The Marx was triggered with a simple trigatron arrangement in the first spark gap. A Kel-F insulator was used first, but was unable to withstand the heat generated during rep-rate operation. A Macor insulator was used subsequently. The trigatron was driven by a MOSFET trigger circuit with an EG&G pulse transformer. The Marx was charged with a positive power supply, so the trigger was arranged to provide a negative pin bias.

When the Marx was first tested we found it difficult to trigger reliably and it exhibited a very slow risetime, even right at the threshold of self-breakdown. This was attributed to not enough stray stage-to-ground capacitance, so discrete capacitance to ground was added to the first three stages, with values decreasing from about 440 pF to 150 pF. This appeared to resolve the problem and adding capacitance to additional stages provided no additional improvement.

### III. BASIC OPERATION

The Marx was first tested in a basic bench-top setup which was already in place for other systems. A Maxwell 4 kJ/sec capacitor charging supply was used to charge the marx. We found that the most consistent diagnostic measurement for characterizing the marx output was a current measurement using a low-resistance high-bandwidth coaxial CVR. For all of the measurements we report, the current was measured with a T&M research 0.05  $\Omega$  CVR with 800 MHz bandwidth. The CVR was plugged directly into the output HV of the marx and the signal was recorded via a Nanofast OP-300 high-bandwidth fiber optic link. The measured risetime response of the link was about 1 ns and was the limiting bandwidth factor in our measurements.

Short circuit measurements were made with the Marx to establish a baseline of operating parameters without risking significant high voltage problems. The Marx was positioned about 9" above a ground plane and shorted to the ground with heavy ground braid. For these measurements, we used the 2.7 nF capacitors and the spark gap spacing was set to about 1.9 mm to reduce the lower extreme of the Marx operation. We found the marx would trigger reliably down to about 5 kV/stage (125 kV o.c.) at atmospheric pressure with compressed dry air.

Figure 2 shows a typical measured waveform at 80 PSI, corresponding to about 30 kV self-breakdown. The waveforms were so consistent that this curve was averaged over 10 individual shots to help reduce the noise introduced by the fiber optic link.

The expanded curve shows the typical damped sinusoid we would expect. The Marx rings at a center frequency of about 9 MHz and damping time constant of about 500 ns. Not surprisingly, we found that the resonant frequency remained fixed as we varied the charging voltage, but the Q increased with voltage, presumably because the hotter spark channels were less resistive. The erected capacitance of this Marx was about 220 pF, so the

resonant frequency corresponds to an overall loop inductance of about 1.4  $\mu\text{H}$ .

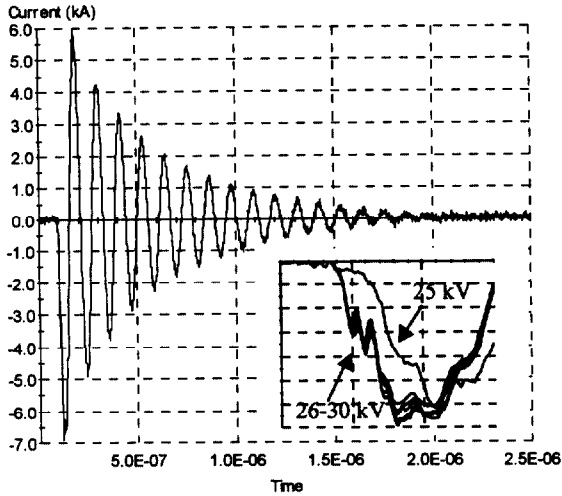


Figure 2. Short circuit current for the marx with 2.7 nF capacitors. The graph shows the current for a charging voltage of 30 kV. The inset graph shows the initial rising edge on an expanded time scale (25 ns per div) for charging voltages ranging from 25 to 30 kV in 1 kV steps.

The inset of Fig. 2 shows the initial rising edge of the current for charging voltages ranging from 25 to 30 kV. The risetime was relatively slow due to the large loop created by the Marx offset from the ground plane. However, the important result shown in this curve is that the Marx triggers very consistently until the top charge voltage drops to 25 kV, at which point a large delay develops. This showed that after the discrete stage capacitance was added we could operate the Marx well away from self-break and be confident that we would have reliable operation without risking pre-triggering.

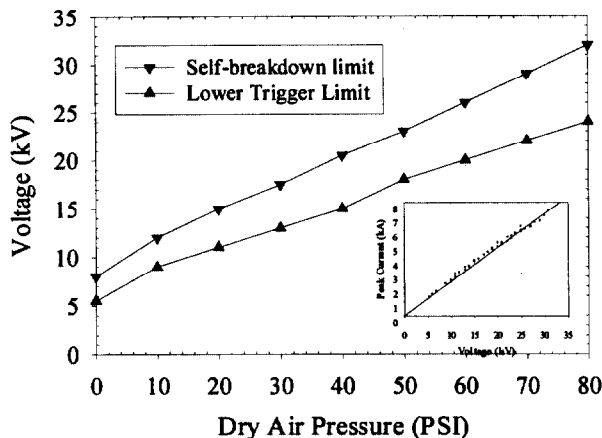


Figure 3. Measured operating limits for marx with 2.7 nF capacitors and 1.9 mm spark gap spacing. The inset graph shows the peak current values at all measured charging voltages.

Figure 3 shows a graph of operating limits of this Marx as a function of the dry air pressure. The upper curve

corresponds to the self-breakdown voltage, while the lower curve shows the minimum triggerable limit, with no regard to risetime speed. The inset of Fig. 3 shows the peak current level versus charging voltage for all measured waveforms. There is some overlap because the same charging voltage was often measured at several different pressures. The graph is linear and again shows the reliability of the Marx performance.

## IV. MODELING

We obtained a copy of a circuit model which the Naval Postgraduate School (NPS) was using to model this Marx design and we modified it for our purposes to compare with experimental results. Fig. 4 shows one stage of the model implemented with MicroCap™. The entire Marx is modeled by chaining this stage 25 times. NPS investigated voltage-dependent switches to model spark gap triggering, but found that the calculation was unstable. Instead, the switches are turned on with a fixed 300 ps delay from stage-to-stage.

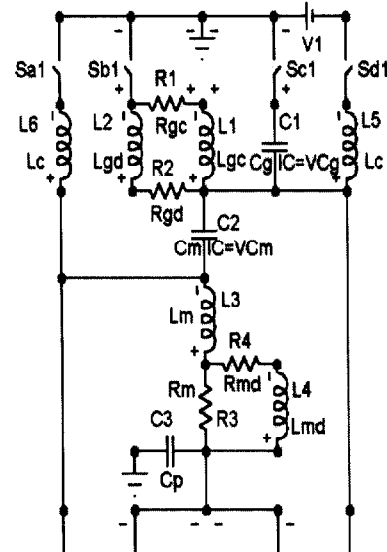


Figure 4. Single stage circuit model of Marx generator.  $C_p$  is the stage to ground capacitance,  $C_m$  is the stage capacitance.

The model includes a fairly simple passive element approach to account for the inductive and resistive stages of spark gap closure, as well as stray capacitance to ground and any effects which might be introduced by the inductive charging method.

Figure 5 shows a comparison between the measured and modeled Marx output. This Marx was populated with the 2 nF capacitors, had 3 mm gap spacing, and was charged to 15 kV for this measurement. A coaxial ground return was provided to investigate the effects of stray capacitance and to explore effects on the risetime. The better geometry decreased the current risetime to between 3 and 4 ns. The decreased loop inductance and decreased erected capacitance (160 pF) combine to increase the Marx self-resonance frequency to about 14 MHz. From

these values the Marx inductance is calculated to be about 800 nH. The predicted impedance from this value would be 70  $\Omega$ , which matches well to the value obtained by the ratio of open circuit voltage (375 kV) to short circuit peak current (5 kA) of 75  $\Omega$ . The model is seen to provide excellent agreement with the measured data. The important adjustable model parameters were the stray stage capacitance, which was chosen to have a value of 6 pF, and the spark gap on-state resistance, which was chosen to be 0.2  $\Omega$ . The resistance primarily affected the damping time-constant and the capacitance had a strong influence on the matching of the general characteristics in the first few resonant cycles.

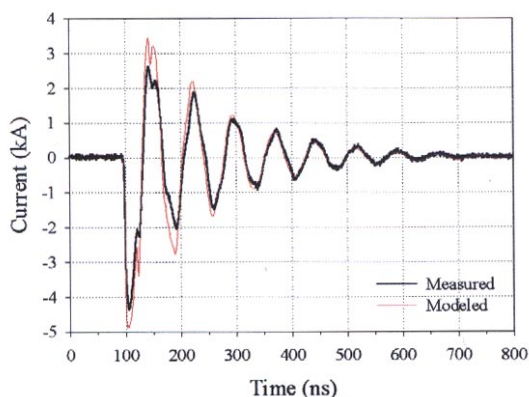


Figure 5. Comparison between modeled and measured results for coaxially shorted Marx generator using 2 nF capacitors and 3 mm gap spacing at 15 kV charge.

Figure 6 shows similar results for the same Marx generator, but with the coaxial short removed and replaced with a distributed 100 ohm load. The only change to the model was to decrease the stray capacitance value from 6 pF to 1 pF to account for the lack of a nearby ground during charging. The measured and modeled current corresponds to about half of the open circuit voltage appearing across the load, and indicates that the internal impedance of the Marx in this configuration is about 100  $\Omega$ . This may be due to two factors: increased inductance because of the restricted current path in the resistive load, and the decreased stray capacitance.

We do not have space in this paper to present more data, but this model was not generally applicable to the Marx behavior. It did not accurately predict the change in Q as the charge voltage is varied because of the simple resistive model of the spark gaps. We examined a more complicated arc model with current dependent impedance

but had stability problems with MicroCap™. The model also had difficulty handling inductive loads.

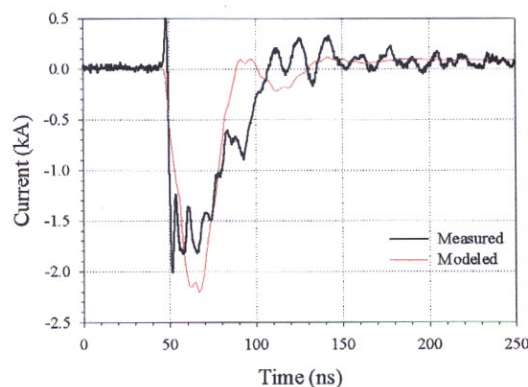
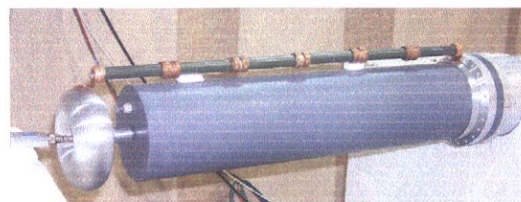


Figure 6. Comparison between modeled and measured results for 100 $\Omega$  distributed load.

Further, we made rep-rate measurements with this Marx and showed that the inductive charging method was satisfactory to operate at up to 50 Hz with consistent results. We found that we were limited by power supply capability not spark gap recovery.

## V. CONCLUSIONS

We described in this paper the construction characteristics and operating behavior of a 1 MV Marx bank generator based in large part on a design from Los Alamos National Laboratory. The Marx is compactly packaged and operates reliably down to about 80% of self-breakdown. Measurements showed that modeling efforts for this Marx are fruitful, but without a better spark gap model fitting parameters will always be required.

## VI. REFERENCES

- [1] A.W. Obst, D. Fulton, N.S.P. King, D.Oro, D. Platts, D.S. Sorenson, M. Stelts, "Performance of the Multi-Pulse X-Ray Imaging System for the Pulsed Power Hydrodynamic Experiments at LANL," Proc. IEEE Pulsed Power Conference, 1997, pp. 448-453.
- [2] K.H. Schoenbach, A. Abou-Ghazala, T. Vithoulkas, R.W. Alden, R. Turner, S. Beebe, "The Effect of Pulsed Electrical Fields on Biological Cells," Proc. IEEE Pulsed Power Conference, 1997, pp. 73-79.